ELSEVIER

Biochimica et Biophysica Acta 1586 (2002) 316–330

BIOCHIMICA ET BIOPHYSICA ACTA

BBA

www.bba-direct.com

# Molecular and functional characterization of a new X-linked chronic granulomatous disease variant ($X91^+$) case with a double missense mutation in the cytosolic gp91*phox* C-terminal tail

Marie José Stasia [a,*], Bernard Lardy [a], Andres Maturana [b], Pascale Rousseau [a], Cécile Martel [a], Pierre Bordigoni [c], Nicolas Demaurex [b], Françoise Morel [a]

[a] *GREPI EA 2938 UJF, Laboratoire d'Enzymologie, CHU 38043 Grenoble Cedex 9, France*

[b] *Department of Physiology and Fondation pour Recherches Médicales, Geneva, Switzerland*

[c] *Service de Médecine Infantile, CHU, Nancy, France*

Received 11 December 2000; received in revised form 3 December 2001; accepted 10 December 2001

**Abstract**

We report here two atypical cases of X-linked CGD patients (first cousins) in which cytochrome $b_{558}$ is present at a normal level but is not functional ($X91^+$). The mutations were localized by single-strand conformational polymorphism of reverse transcriptase–polymerase chain reaction amplified fragments and then identified by sequence analysis. They consisted in two base substitutions (C919 to A and C923 to G), changing His303 to Asn and Pro304 to Arg in the cytosolic gp91*phox* C-terminal tail. Mismatched polymerase chain reaction and genomic DNA sequencing showed that mothers had both wild-type and mutated alleles, confirming that this case was transmitted in an X-linked fashion. A normal amount of FAD was found in neutrophil membranes, both in the $X91^+$ patients and their parents. Epstein–Barr virus-transformed B lymphocytes from the $X91^+$ patients acidified normally upon stimulation with arachidonic acid, indicating that the mutated gp91*phox* still functioned as a proton channel. A cell-free translocation assay demonstrated that the association of the cytosolic factors p47*phox* and p67*phox* with the membrane fraction was strongly disrupted. We concluded that residues 303 and 304 are crucial for the stable assembly of the NADPH oxidase complex and for electron transfer, but not for its proton channel activity. 

*Keywords:* Chronic granulomatous disease; Missense mutation; Cytochrome $b_{558}$; NADPH oxidase; Cytosolic factor translocation; FAD binding site

Abbreviations: BCECF-AM, biscarbonyl cyanide *m*-chlorophenyl-hydrazone; CGD, chronic granulomatous disease; CCCP, carbonyl cyanide *m*-chlorophenyl-hydrazone; DPI, diphenylene iodonium; PBS, phosphate-buffered saline; EBV, Epstein–Barr virus; PMN, polymorphonuclear neutrophil; PMSF, phenylmethylsulfonyl fluoride; EDTA, ethylenediaminetetraacetic acid; EGTA, ethylene glycol-bis(β-aminoethyl ether)-*N*,*N*,*N*′,*N*′-tetraacetic acid; FMLP, formyl methionyl-leucyl-phenylalanine; HRP, horseradish peroxidase; NBT, nitroblue tetrazolium; PAGE, polyacrylamide gel electrophoresis; PCR, polymerase chain reaction; PMA, phorbol myristate acetate; RT, reverse transcriptase; SDS, sodium dodecyl sulfate; TLCK, tosyl lysyl-chloromethyl ketone

* Corresponding author. Fax: +33-4-7676-5608.

*E-mail address:* mjstasia@chu-grenoble.fr (M.J. Stasia).

0925-4439/02/$ – see front matter 
PII: S0925-4439(01)00110-7

## 1. Introduction

In response to a wide range of stimuli, phagocytic cells produce reactive oxygen intermediates which have an important role in host defense. NADPH oxidase from phagocytes and nonphagocytic cells such as Epstein–Barr virus-immortalized (EBV) B lymphocytes is responsible for superoxide $O_2^-$ production [1]. In resting cells, NADPH oxidase lacks activity. Oxidase activation needs the assembly at the membrane level of at least five different protein factors. In fact, during the course of neutrophil stimulation, the cytosolic factors p47*phox*, p67*phox*/p40*phox*, and Rac1/2 translocate to the plasma membrane and associate with cytochrome $b_{558}$ [2–7]. Cytochrome $b_{558}$ is a hemoprotein consisting of two α (p22*phox*) and β (gp91*phox*) subunits: this is the redox oxidase center and catalyzes the electron transfer from NADPH to oxygen. It binds two hemes [8]. Gp91phox functions as a flavodehydrogenase and has certain sequence analogies with the ferredoxin-$NADP^+$ reductase (FNR) [9–11], suggesting the presence of both NADPH and FAD-binding domains, as demonstrated by photolabeling experiments [9,12,13].

Similar to mitochondrial cytochromes, gp91*phox* conducts protons to compensate for the charge generated by electron transfer across the plasma membrane [14,15]. The recent report showing that inward $H^+$ currents are absent in cells from an $X91^0$ patient suggested that gp91*phox* behaves as an unusual $H^+$ channel that allows $H^+$ influx and cytosolic acidification [16]. However, because the inward $H^+$ currents did not correlate with oxidase activity, it was recently proposed that gp91*phox* is not an $H^+$ channel but instead modulates preexisting channels [17]. Expression of full-length or *N*-truncated gp91*phox* and mutagenesis experiments were consistent with gp91*phox* being the $H^+$ channel itself [18–21]. Furthermore, the recently cloned NADPH oxidase homologues NOX-1 and NOX-5 also function as $H^+$ channels [22,23]. $H^+$ conduction was mapped to a histidine repeat within the third transmembrane domain, with the central residue (His 115) being critical for both $H^+$ conduction and heme ligation [24]. This suggests that, during oxidase assembly, structural changes occur within the gp91*phox* cytochrome that modulate its $H^+$ channel activity and generate inward $H^+$ currents.

Chronic granulomatous disease (CGD) is a rare inherited disorder in which phagocytic cells are unable to generate superoxide anions. Patients with CGD are predisposed to recurrent bacterial and fungal infections because of the absence of $O_2^-$-generating NADPH oxidase activity [25–27]. There are four types of CGD that make up the autosomal forms with mutations in the genes encoding p47*phox*, p67*phox*, or p22*phox* proteins and the most common X-linked CGD type (approximately 75%), with defects in the *CYBB* gene encoding gp91*phox* where cytochrome $b_{558}$ is absent ($X91^0$) [28–31]. Several types of mutations of gp91*phox* have been reported in X-linked CGD, including deletional, insertional, splicing, missense, nonsense, and duplicational mutations [30]. In a very few rare cases, missense mutations resulting in normal but nonfunctional levels of cytochrome $b_{558}$ have been identified ($X91^+$) [32–42]. Some of these have provided interesting information about the NADPH oxidase structure and activation mechanisms. Two of these $X91^+$ CGD patients had missense mutations leading to substitutions (Arg54 to Ser and Ala57 to Glu) in the N-terminal region of gp91*phox*, which affect heme binding and/or stable interaction with p22*phox* [32,33]. The other functional defects in the CYBB gene were related to mutations in the C-terminal tail of gp91*phox*, which contains the putative FAD and the NADPH binding sites and cytosolic factor interaction domains [34–37].

We report here two new CGD cases of the $X^+$ type identified in first cousins, whose neutrophils fail to produce $O_2^-$ but contain cytochrome $b_{558}$. The functional defect was identified as a double missense mutation substituting His303 to Asn and Pro304 to Arg in the gp91*phox* cytosolic C-terminal tail near the putative FAD-binding domain. We demonstrate that the reversal of charges in the cytochrome $b_{558}$ disturbed the assembly of the NADPH oxidase complex and is critical for the electron transfer from NADPH to $O_2$. In contrast, the mutated cytochrome $b_{558}$ has a normal FAD-binding capacity and is still able to function as an $H^+$ channel and to catalyze cytosolic acidification.

## 2. Materials and methods

### 2.1. Materials

Phorbol 12-myristate 13-acetate (PMA), formyl methionyl leucyl phenylalanine (fMLP), and cytochrome *c* (horse's heart, type VI) were purchased from Sigma Chemical Co. (St Louis, MO, USA). Diisopropyl fluorophosphate (DFP) was purchased from Sigma–Aldrich (Lisle d'Abeau Chesnes, France). NADPH, avian myeloblastosis virus reverse transcriptase, and Taq DNA polymerase were from Roche Molecular Biochemical (Meylan, France). Reagents and molecular mass markers for SDS–PAGE came from Amersham (Buckinghamshire, UK). Nitrocellulose sheets for Western blotting were purchased from BioRad Laboratories (Richmond, CA, USA). Trizol reagent was from Life Technologies (Gaithersburg, MD, USA). Monoclonal antibodies (mAbs) 449 and 48 were kindly provided by Drs. Roos and Verhoeven in Amsterdam. The synthetic peptide VITKVVT**HP**FKTIE (residues 296–309 of the gp91*phox* sequence) and the peptide VITKVVT**NR**FKTIE, containing the double substitution as predicted in patient JR, were purchased from Neosystem (Strasbourg, France) and were more than 95% pure as controlled by high-performance liquid chromatographic analysis. They were dissolved in PBS to a concentration of 2 mM and kept at −20°C.

### 2.2. Case report

Patient JR is a boy who, at the age of 9 months, presented a reaction due to Calmette–Guérin bacillus with associated axillary lymphadenitis. When he was 8 years old he developed a liver abscess caused by *Staphylococcus aureus* and CGD was diagnosed by the absence of NBT reduction in neutrophils. A prophylactic treatment with sulfamethoxazole, trimethoprime, and itraconazole was given, which prevented new infections. To investigate the neutrophil response in both parents, the NBT slide test was used: it was normal in the father and gave intermediate values in the mother (50% of total neutrophils were not able to reduce the NBT), both of them being in good health. The first cousin (on the maternal side) of the same age, patient VV, presented a similar clinical story and CGD was also diagnosed at 8 years of age. His mother had the same NBT slide test result as patient JR's mother. The two boys are now 16 years old.

### 2.3. Cell preparations

Human neutrophils and mononuclear cells (lymphocytes plus monocytes) were isolated from 25 ml of citrated blood from patients JR and VV, their parents, and normal volunteers as described [43], after having obtained their informed consent. Lymphocytes from 5 ml of heparinized sterile venous blood were collected by Ficoll–Hypaque density gradient centrifugation and infected with the B95-8 strain of EBV as previously described [44]. The EBV-B lymphocyte cell line was grown in RPMI-1640 supplemented with 10% fetal calf serum, 100 U/ml penicillin, 50 μg/ml kanamycin and 50 μg/ml streptomycin, at 37°C in a 5% $CO_2$ atmosphere.

### 2.4. Superoxide assay

NADPH oxidase activity of intact neutrophils was assessed by measuring the rate of superoxide sensitive cytochrome *c* reduction at 550 nm in presence of SOD ($\varepsilon_{550}$ 21.1 $mM^{-1}\,cm^{-1}$) [44].

### 2.5. Preparation of RNA and DNA

Total RNA was isolated from both native mononuclear cells and EBV-transformed B lymphocytes of CGD patients as well as healthy donors, with a modified single-step method described in [45] using Trizol reagent.

Genomic DNA was purified from mononuclear cells and EBV-transformed B lymphocytes of CGD patients and normal subjects following classic procedures [46].

### 2.6. cDNA amplification

First-strand cDNA synthesis was performed from total RNA in 20 μl containing RT buffer, using oligo-dT primers or for specific reverse transcription using primer 12* (Table 1) and a cDNA synthesis kit according to the manufacturer's instructions (Appligen Oncor, Illkirch, France). The cDNA was im-

mediately amplified by PCR. In some experiments, commercial actin primers were run in parallel with PCR tests as a control for PCR and RNA extraction efficiency. Aliquots of 10-μl PCR products in bromophenol blue solution were run together with a scale of DNA ladders (markers VI, Boehringer Mannheim, Meylan, France) on 1.5% (w/v) agarose gels containing 1 μg/ml ethidium bromide. The bands were photographed under UV using Polaroid films.

### 2.7. Sequencing of the PCR products

PCR products were gel-purified and sequenced by Genome Express, Grenoble, France, with forward and backward primers using the Abi Prism automatic sequencer (Perkin Elmer, Courtaboeuf, France). PCR products were obtained from cDNA or genomic DNA of patients JR and VV and their parents from native mononuclear cells and from EBV-B lymphocyte cell lines.

### 2.8. SSCP analysis

RT–PCR products were diluted twice with SSCP loading buffer (20 mmol/l EDTA, 90% (v/v) formamide, 0.1% (w/v) xylene cyanol, 0.1% (w/v) bromophenol blue); they were denatured at 95°C for 5 min and then chilled on ice [47]. The samples were loaded onto a nondenaturing 10% acrylamide gel containing 5% (w/v) glycerol, 0.5× TBE (50 mM Tris–borate, 1 mM EDTA, pH 8) and submitted to electrophoresis at 5 W, and 18°C for 18 h in a BioRad Dcode Universal mutation detection system. The gel was silver stained according to the manufacturer's instructions.

### 2.9. Mismatch PCR

Genomic DNA purified from peripheral blood mononuclear cells or EBV-immortalized B lymphocytes was amplified using two pairs of specific primers. One pair of oligonucleotides was composed of a forward primer 13, which is complementary to the wild-type sequence of gp91*phox* cDNA, and a backward primer 15*. The other pair consisted of primer 14, which is complementary to a mutant sequence of gp91*phox* cDNA, and primer 15* (see sequences of primers in Table 1).

### 2.10. Cytochrome $b_{558}$ spectroscopy

Purified neutrophils treated by 3 mM diisopropyl fluorophosphate were lysed for cytochrome $b_{558}$ extraction with a buffer containing 1% (w/v) Triton X-100, 10 mM HEPES, 3.5 mM $MgCl_2$, 1 mM PMSF, 0.1 mM leupeptin, 1 mM EGTA, and 1 mM EDTA, pH 7.4. After 20 min incubation at 4°C, the lysate was centrifuged at $20\,000 \times g$ for 30 min [48]. The supernatant was used for the immunoblotting experiment and cytochrome $b_{558}$ spectroscopy. Reduced minus oxidized differential absorption spectra were recorded at room temperature with a DU 640 Beckman spectrophotometer [49]. A molecular extinction coefficient of $\varepsilon_{426-410\,nm} = 200\ mM^{-1}\,cm^{-1}$ for the Soret band was used for calculations.

### 2.11. Determination of flavin content in membranes

Neutrophil membranes were diluted in a 50 mM sodium/potassium phosphate buffer. The membrane suspension was boiled for 3 min, then put on ice to liberate FAD. After centrifugation, the supernatant

Table 1
Sequence of oligonucleotide primers used for the PCR amplification of gp91*phox* cDNA and genomic DNA

| Primers | Sequence | Position |
|---|---|---|
| 1 | CCTCTGCCACCATGGGGAAC | 2 |
| 2* | GTGAATCGCAGAGTGAAGTG | 357 |
| 3 | GAGTTCGAAGACAACTGGAC | 278 |
| 4* | GACTTCAAAGTAAGACCTCCGGATG | 624 |
| 5 | GCATCACTGGAGTTGTCATCA | 539 |
| 6 | CTATGACTTGGAAATGGATAG | 812 |
| 7* | CAACGATGCGGATATGGATAC | 1087 |
| 8* | CCACCTCATAGCTGAACACA | 1222 |
| 9 | ATAAGCAGGAGTTTCAAGAT | 1127 |
| 10* | GAGGTAGATGTTGTAGCTGAG | 1452 |
| 11 | GCAGATCTGCTGCAACTGC | 1375 |
| 12* | TTTCCTCATGGAAGAGACAAG | 1746 |
| 13 | GTGGTCACTCACCCTTTCAAAAC | 910 |
| 14 | GTGGTCACTAACCGTTTCAAAAC | 910 |
| 15* | AGGTAGTTTCCACGCATCTTG | 1161 |
| 16 | GAAAAATGTCATTTCCAGACATATG | Intron 8 |

Pairs of oligonucleotides (1,2*), (3,4*), (6,7*), (9,10*), (11,12*) were used as primers for PCR amplification and SSCP analysis. Pair (5,8*) was also used in this experiment, except that the PCR product was digested with restriction enzyme *Mae*III. Oligonucleotides 13, 14, and 15* were used as primers for mismatch PCR and primers (16,7*) for PCR amplification of exon 9's part from genomic DNA. *Anti-sense strand.

was diluted twice in 0.2 M borate buffer (pH 9), and 0.5 mU phosphodiesterase was added to generate FMN from FAD in a final volume of 100 μl at room temperature. In 10 min, FAD was totally hydrolyzed in FMN. After 15 and 30 min of hydrolysis, aliquots were analyzed for FMN by chemiluminescence reaction in a medium containing 70 μM 2-mercaptoethanol, 50 μM decylaldehyde, and 100 μM NADH in 50 mM phosphate buffer, pH 6.8 [50]. Desalted luciferase was added and RLU counts were monitored at 30°C in a Luminoscan luminometer (Labsystems, Helsinki, Finland) coupled with a computer. A standard curve in the range of 0.1–100 pmol of FMN was performed. We were able to measure the amount of membrane-bound FAD in $5.10^5$ cell-equivalent accurately using this method. The amount of FMN measured without addition of phosphodiesterase was less than 4% of total flavins.

### 2.12. Cytosolic pH measurements

EBV-transformed B lymphocytes were suspended at a concentration of $2\times10^6$ cells/ml in $Na^+$ medium (150 mM NaCl, 1 mM KCl, 5 mM HEPES, 5.5 mM glucose, pH 7.3), incubated with 5 μM BCECF-AM for 20 min at room temperature, centrifuged (5 min at 1000 rpm), and resuspended in the $Na^+$ medium. $H^+$ channel activity was assessed as described [19] by measuring BCECF ratio fluorescence, using a Jasco CAF-110 fluorescence spectrometer (Hachioji City, Japan) and alternate excitation at 490 and 455 nm. To prevent $Na^+/H^+$ exchange and NADPH oxidase-mediated acidification and to clamp the membrane potential, 0.3 mM amiloride, 5 μM DPI, and 2.7 μM valinomycin were included. The $H^+$ channel was then activated by arachidonic acid (8 μM) and an inward proton gradient was imposed by adding 10 mM HEPES in order to decrease the extracellular pH to 6.6. At the end of the experiment, 50 μM CCCP was added to equilibrate the cytosolic pH ($pH_i$) with the external pH, and a calibration curve was performed to convert the ratio traces into $pH_i$ values.

### 2.13. Cell-free superoxide-generating system

NADPH oxidase activity was reconstituted through a homologous cell-free assay [44]. Briefly, neutrophil membranes (30 μg) were mixed with cytosol (300 μg) in PBS buffer containing 20 μM GTPγS, 5 mM $MgCl_2$ and arachidonic acid in a final volume of 100 μl. Peptides (296–309 and 491–504) at a final concentration from 0 to 60 μM were added in the medium of cell-free assay 2 min before addition of arachidonic acid as described in [36]. A preliminary assay was performed to determine the optimal amount of arachidonic acid necessary to provide maximal oxidase activation. After incubation for 10 min at 25°C, the oxidase activation medium was transferred into a spectrophotometric cuvette containing 100 μM cytochrome *c*, and the reaction was then initiated with 150 μM NADPH (final volume 1 ml).

### 2.14. Cytosolic protein translocation in the cell-free system

Plasma membranes and cytosol were obtained from purified neutrophils as described before [49]. NADPH oxidase activity was reconstituted through a homologous cell-free assay. Briefly, neutrophil membranes (30 μg) were mixed with cytosol (300 μg) in oxidase buffer as described in [36]. SDS (100 μM) and GTPγS (10 μM) were added (final volume 1 ml) and after 10 min at room temperature the mixture was loaded on a discontinuous sucrose gradient. After centrifugation (1 h, 30 000 rpm, in an SW41 rotor (Beckman) at 18°C), the membranes were collected between the two 45% and 20% (w/v) sucrose layers and analyzed by immunoblotting with specific antibodies directed against cytosolic proteins as described in the following section.

### 2.15. SDS–PAGE and immunoblotting

Proteins solubilized in a 1% Triton X-100 from neutrophils were separated by SDS–PAGE in 10% (w/v) acrylamide gel with a 5% (w/v) stacking gel [51], electrotransferred to nitrocellulose [52] and immunodetected by monoclonal antibodies mAbs 449 and 48 directed against p22*phox* and gp91*phox*, respectively [53], or polyclonal anti-peptide antibodies directed against p47*phox* and p67*phox* proteins [54]. Detection was mediated with HRP-labeled goat anti-rabbit or anti-mouse IgG followed by a chemiluminescence reaction. The film's exposure was less than 1 min.

### 2.16. Protein determination

The protein content was estimated using the Bradford assay [55].

## 3. Results

### 3.1. CGD diagnosis of patients JR and VV

The neutrophils of patient JR, stimulated with PMA and fMLP, showed no respiratory burst as measured by the SOD-sensitive cytochrome *c* reduction assay (Table 2). Neutrophils from JR's father had a normal NADPH-oxidase activity and those from his mother gave intermediate values. Neutrophils from the first cousin, patient VV, and his parents showed similar results (data not shown). The NBT-slide test confirmed previous observations and the mode of inheritance supported an X-linked mutation. To determine the X-linked CGD type in patient JR, we measured the cytochrome $b_{558}$ content of a 1% Triton X-100 soluble extract (50 μg of proteins in each sample) from neutrophils using reduced minus oxidized difference spectroscopy. As illustrated in Fig. 1A, the differential spectrum revealed a normal amount of cytochrome $b_{558}$ (110 pmol/mg) in patient JR's neutrophils, similar to the neutrophil membrane extract's spectrum from a healthy donor (140 pmol/mg (curve b versus curve a)) and in contrast to the spectrum of $X^0$ CGD neutrophils in which the γ, β, and α peaks of cytochrome $b_{558}$ were absent (Fig. 1, curve c).

Table 2
NADPH oxidase activity in intact neutrophils from the $X91^+$ CGD patient JR and his parents

| | $O_2^-$ generation nmol $O_2^-$/min/$10^6$ cells | |
|---|---|---|
| | fMLP | PMA |
| Patient JR | 0 | 0 |
| Patient JR's mother | 6.0 | 9.4 |
| Patient JR's father | 13.3 | 23.3 |
| Control ($n=5$) | 10.8 ± 3.1 | 17.8 ± 2.5 |

Neutrophils ($1\times10^6$ cells in PBS) were stimulated with PMA (20 ng/ml) or with fMLP ($10^{-7}$ M) and $O_2^-$ generation was determined by superoxide dismutase-inhibitable cytochrome *c* reduction assay, as described in Section 2. Control data represent mean ± S.D. ($n=5$).

The presence of membrane components of the NADPH oxidase complex was demonstrated through an immunodetection experiment (Fig. 1B) using an identical amount of 1% soluble extract from purified neutrophils in all samples (50 μg). We illustrated the presence of cytochrome $b_{558}$ in patient JR (lane 2) and his parents' neutrophils (the mother in lane 3 and the father in lane 4), as shown by the two

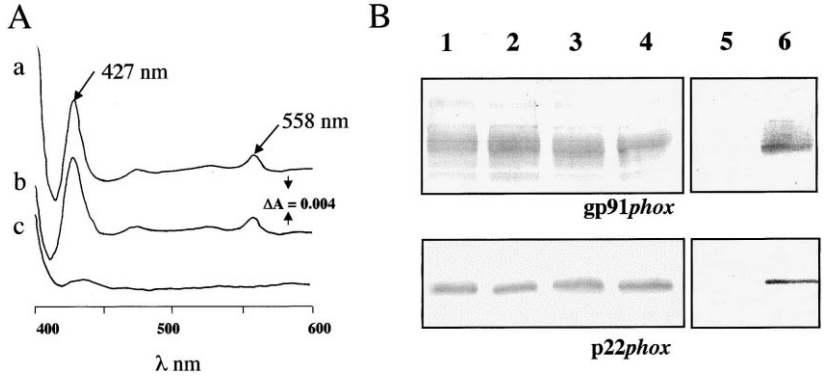


Fig. 1. Reduced minus oxidized difference spectra and immunodetection of cytochrome $b_{558}$ in neutrophils from the $X91^+$CGD patient JR and his parents. The experiment was performed on 1% Triton X-100 soluble extract of neutrophils (50 μg) at room temperature. The absorption profile of reduced minus oxidized spectra is shown for a healthy donor (a), $X91^+$ patient JR (b), and $X91^0$ patient AF (c) from the top (A). Fifty μg of the same 1% Triton X-100 soluble extract from control neutrophils (lane 1), patient JR's neutrophils (lane 2), his mother's neutrophils (lane 3), his father's neutrophils (lane 4), from $X91^0$ CGD patient AF (lane 5), and from control neutrophils again (lane 6), were subjected to SDS–PAGE and blotted onto a nitrocellulose sheet (B). α and β subunits of cytochrome $b_{558}$ were revealed with monoclonal antibodies mAb 449 (α) and mAb 48 (β). This result represents one experiment in five.

α and β subunit bands. The specificity of the monoclonal antibodies directed against the two gp91*phox* subunits was demonstrated by the absence of gp91*phox* and p22*phox* in the $X^0$CGD-soluble extract, seen in lane 5, as compared to the control neutrophil extract (lane 6). A similar experiment was performed with the cytosolic factors p67*phox*, p47*phox*, and p40*phox*, giving an identical ratio in all the samples (data not shown). The results suggest that the phenotype was compatible with a mutation located either in the gene encoding gp91*phox* and leading to a nonfunctional cytochrome $b_{558}$, as found in the $X91^+$ CGD type, or with a defect at an unrelated locus on the X chromosome that encodes an unknown protein critical to the function of NADPH oxidase.

### 3.2. Genetic analysis of CGD patients JR and VV

SSCP analysis was performed to localize the mutation in the mRNA encoding gp91*phox*. The control's and the patient's mRNAs were reverse-transcribed into six overlapping cDNA fragments with six pairs of oligonucleotide primers derived from the gp91*phox* cDNA (Table 1) and were studied by SSCP analysis. In only two of them migration was abnormal (Fig. 2A,B). Fragment 1 (residues 812–1087), obtained with primers 6 and 7* (Table 1) and localized in exon 9 of the *CYBB* gene (Fig. 2A), demonstrated an abnormal electrophoretic migration shift for patient JR (lane 3) and for his first cousin, patient VV (lane 4), compared to the control (lane 2). The same fragment amplified from the $X^0$CGD patient AF with a nonsense mutation in exon 9 (unpublished data) also had an abnormal migration (lane 1). In order to ascertain this first result, the migration of fragment 2 (residues 539–1222), amplified with primers 5 and 8* (see Table 1), which include fragment 1's sequence, was analyzed with the same procedure (Fig. 2B). This second fragment also had an abnormal mobility shift for patient JR (Fig. 2B, lane 2) compared to the migration of a fragment amplified from a healthy donor (Fig. 2B, lane 1).

These two RT–PCR fragments from patient JR and patient VV were gel-purified and sequenced with two pairs of forward and backward oligonucleotide primers. In both fragments, two base substitutions were similarly detected (C919 to A and C923 to G), changing His303 to Asn and Pro304 to Arg, in the gp91*phox* cytosolic C-terminal tail, in a region near the putative FAD-binding domain (Fig. 3A). We also sequenced all the gp91*phox* cDNA of patients JR and VV from the four other fragments and we found no other point mutations. The double mutation was also found in both strands of the genomic DNA from patient JR and patient VV by PCR amplification and sequencing, using forward primer 16 derived from the intron 8 sequence end (Dinauer, personal communication) and backward primer 7* localized in exon 9 (sequences seen in Table 1). As seen in Fig. 3B, patient JR was hemizygous for the mutations as compared to his father's genomic DNA sequence. For his mother, the double mutation was present in one of the two alleles with the presence of both bases C and A at position 919 and bases C and G at position 923. The same results were obtained from patient VV and his parents. In parallel, 50 control genomic DNA were checked and no mutations were found, as for both patients' fathers.

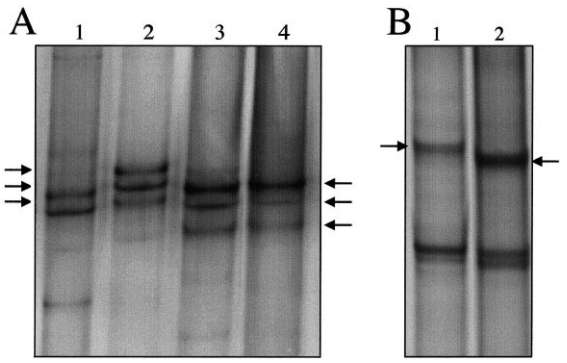


Fig. 2. SSCP analysis of the amplified gp91*phox* cDNA fragments. (A) SSCP analysis of PCR-amplified fragment 1 obtained with oligonucleotides (6,7*) from $X91^0$ CGD patient AF with a nonsense mutation in a site very close to patient JR's mutations (lane 1, unpublished data), from a healthy donor (lane 2), from patient JR (lane 3), and from patient VV (patient JR's first cousin) (lane 4). (B) SSCP analysis of the PCR amplified fragment 2 obtained with the oligonucleotides (5,8*). Fragment 2 was digested with the restriction enzyme *Mae*III just before electrophoresis, from a healthy donor (lane 1) and from $X91^+$ CGD patient JR (lane 2). The sequence of fragment 1 (A) was enclosed in the sequence of fragment 2 (B). The arrow indicates the shift of the cDNA fragments.

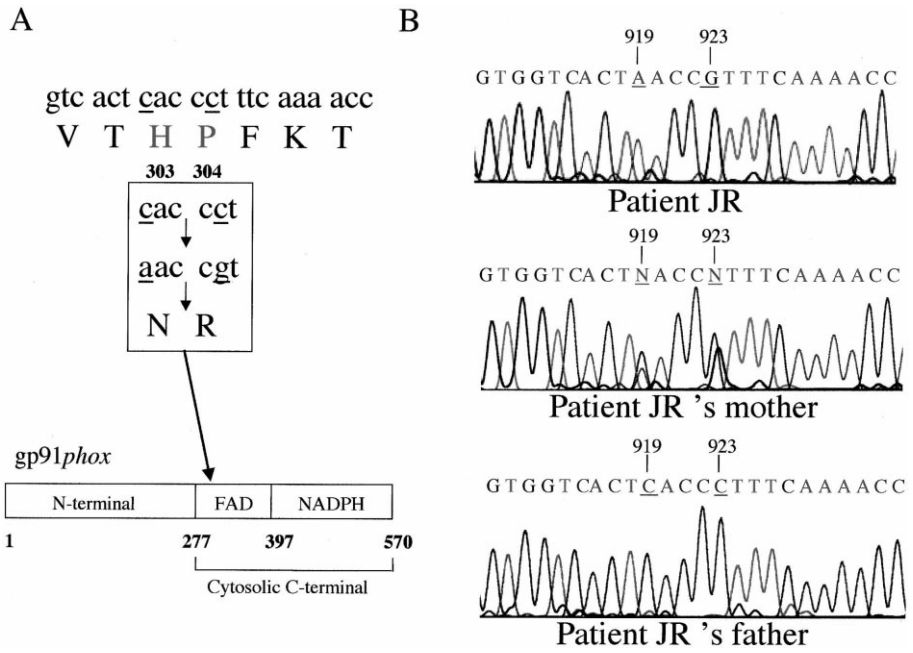


Fig. 3. Analysis of mutations in gp91*phox* mRNA and in the *CYBB* gene. RT–PCR products were gel-purified and automatically sequenced by Genome Express, Grenoble, France, with forward and backward primers (5,8*) and (6,7*) (sequences seen in Table 1) as described in Section 2. A double mutation was detected, changing His303 to Asn and Pro304 to Arg in the gp91*phox* cytosolic C-terminal tail containing putative FAD- and NADPH-binding domains, as seen in A. RT–PCR products were obtained and sequenced from patients JR and VV's EBV-B lymphocytes and native mononuclear cells. Mutations were confirmed by genomic DNA PCR amplification and sequencing using the primers (16,7*) described in Table 1. ND, nondetermined nucleotide due to the presence at the same position of two different bases.

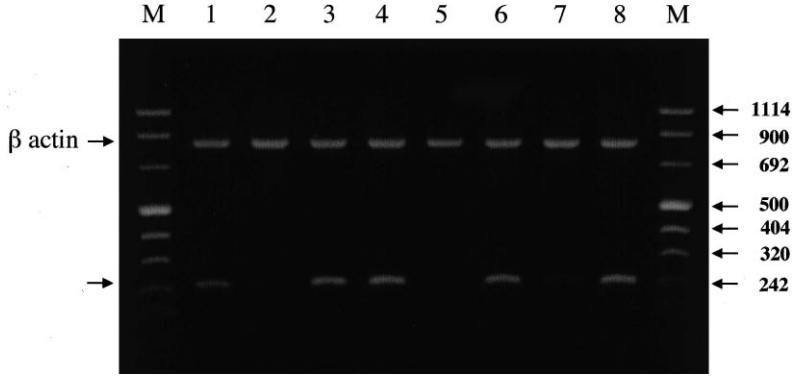


Fig. 4. Mismatch PCR of genomic DNA from patient JR and his parents. Primers 14 and 15* were used in lanes 1, 3, 5, 7 and primers 13 and 15* in lanes 2, 4, 6, 8 (see Table 1 for sequences and positions). M, molecular markers. The PCR product was detected only when primer 13 and primer 15* were used in genomic DNA prepared from peripheral blood mononuclear cells from the father (lanes 5, 6) and from a healthy adult (lanes 7, 8). On the other hand, in genomic DNA from the patient's mononuclear cells (lanes 1, 2), the PCR product was detected only when primer 14 and primer 15* were used. In genomic DNA from the mononuclear cells from the mother (lanes 3, 4), the PCR product was detected when either primer 13 and primer 15* or primer 14 and primer 15* were used. Mismatch PCR was also performed with purified genomic DNA from 50 healthy donors and no amplification occurred with primers 14 and 15*. The same experiment was performed from genomic DNA from patient VV and his parents.

To confirm that the mutated gene was transmitted from the mother, genomic DNA mismatch PCR was performed using wild-type or mutated forward primers (primers 13 or 14, respectively) and primer 15* as the backward oligonucleotide (Table 1). As shown in Fig. 4, in the case of genomic DNA prepared from patient JR's mononuclear cells (lanes 1 and 2), only the combination containing the mutated primer could produce a 255 bp band, while two 255 bp fragments were produced from the mother's DNA (lanes 3 and 4) with the two pairs of primers. Similarly, a 255 bp fragment was obtained only with the wild-type primer from the father (lanes 5 and 6), as in the control experiment (lanes 7 and 8). This result confirmed that the mutated gene was transmitted from the patient's mother. The same experiment was performed with genomic DNA from patient VV and his parents and from EBV-B lymphocyte cell lines, giving similar results (data not shown). No double mutations were found in all the mismatch PCRs made with control genomic DNA (50 control alleles).

### 3.3. Determination of the flavin content of neutrophil membranes

As the described double mutation was localized upstream but near the putative FAD-binding domain, which begins at Leu335 according to information deduced from sequence alignments of the cytosolic gp91*phox* C-terminal tail with members of the ferredoxin-NADPH reductase family [9–11], we decided to measure the FAD content of neutrophil membranes (Table 3). The amount of FAD was shown to be correlated with that of cytochrome $b_{558}$, as shown by the result of the X91$^0$ patient (21.0 ± 4 pmol/mg protein) compared to controls

Table 3
FAD content in neutrophil plasma membranes

| | FAD | |
|---|---|---|
| | pmol/mg protein | % of control |
| Control | 97 ± 18 | 100 |
| X$^0$ CGD patient AF | 21 ± 4 | 22 |
| X$^+$ CGD patient JR | 84 ± 14 | 87 |
| JR's mother | 105 ± 35 | 108 |
| JR's father | 104 ± 10 | 107 |

Values represent the mean ± S.D. of triplicate determinations. The amount of membrane-bound FAD was measured with $5 \times 10^5$ cell equivalent. Noncovalently bound FAD was measured by the chemiluminescence method described in Section 2.

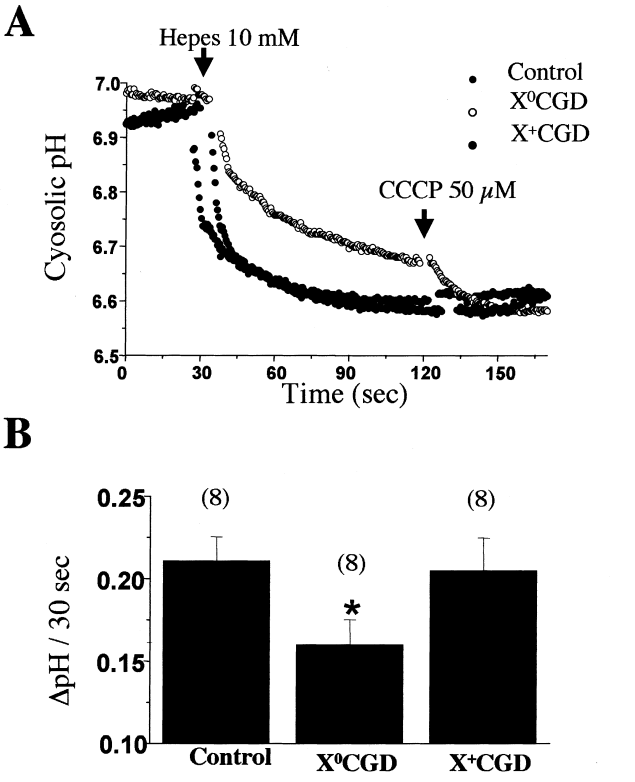


Fig. 5. H$^+$ channel activity in EBV-transformed B-lymphocyte cell lines. Cytosolic acidification in response to an imposed pH gradient was measured with BCECF, as described in Section 2. Cells were incubated with amiloride, DPI, and valinomycin (2.7 μM) and H$^+$ channel activity was initiated with arachidonic acid (8 μM). An inward pH gradient was subsequently imposed by adding 10 mM HEPES to the cell suspension in order to clamp the extracellular pH to 6.6. Superimposed traces showing cytosolic acidification in EBV-transformed B lymphocytes derived from the three patients are shown in A. Cells from the control (dark filled circles) and the X91$^+$ patient (gray filled circles) rapidly acidified to levels close to the external pH. In contrast, cells from the X91$^0$ patient (open circles) acidified more slowly and remained more alkaline than the external pH. The protonophore CCCP (50 μM) was added to equilibrate the cytosolic pH with the external pH. Traces are representative of eight different experiments. In B, the extent of cytosolic acidification measured 30 s after imposing the pH gradient is shown. Data are mean ± S.E.M. from eight independent experiments, performed on three different preparations of EBV-transformed B lymphocytes.

(97 ± 18 pmol/mg protein). The amount of FAD in patient JR's neutrophil membranes (84 ± 14 pmol/mg protein) was as high as that of control membranes and similar to that of neutrophil membranes from his father (104 ± 10 pmol/mg protein) and his mother (105 ± 35 pmol/mg protein). Identical results were obtained with neutrophil membranes from patient VV and members of his family (data not shown).

### 3.4. Cytosolic pH measurement in EBV-transformed B lymphocytes

To assess whether the mutated gp91*phox* protein could still function as a proton channel, we measured cytosolic pH changes in EBV-transformed B lymphocytes derived from patient JR. To selectively measure gp91*phox* $H^+$ fluxes, the oxidase was activated with arachidonic acid in conditions allowing only $H^+$ influx, as described in [19]. An inward proton gradient was imposed by a combination of valinomycin (to clamp the membrane potential) and HEPES (to decrease the external pH to 6.6), and cytosolic pH changes were measured with BCECF in the presence of amiloride (to inhibit $Na/H^+$ exchange) and DPI (to prevent acid production by the oxidase). In these conditions, a cytosolic acidification reflects the oxidase-associated $H^+$ channel activity corresponding to the inward $H^+$ currents measured in patch-clamp studies [16,17]. As shown in Fig. 5A,B, cells from a control patient acidified rapidly upon addition of HEPES, their cytosolic pH equilibrating within 2 min with the external pH (Fig. 5, dark filled circles). As expected from the lack of a gp91*phox* $H^+$ channel, cells from the $X91^0$ patient AF acidified more slowly and their cytosol remained more alkaline than the external pH throughout the experiment (open circles). Cells from the $X91^+$ patient JR acidified with similar kinetics and to the same extent as cells from the control patient (gray filled circles), indicating that the mutated cytochrome retained its $H^+$ channel activity and could still be activated by arachidonic acid. This suggests that the motif required for $H^+$ transport is not affected by the double mutation in the gp91*phox* cytosolic C-terminal tail, consistent with earlier observations in $X91^+$ patients [15] and with expression studies of gp91*phox* truncated mutants [20,21].

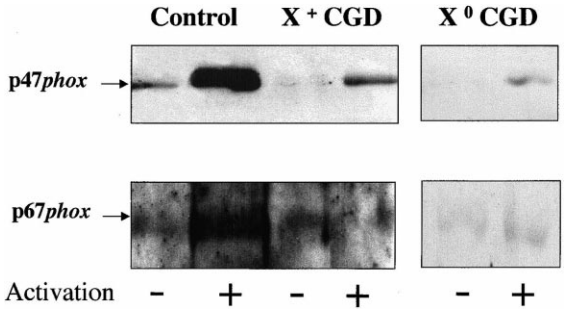


Fig. 6. Western blot analysis of neutrophil membranes isolated after assembling using a cell-free activation assay. Patients or control neutrophil membranes (30 μg) were incubated with control neutrophil cytosol (300 μg) in oxidase buffer at room temperature. After 10 min of incubation in presence (+) or in absence (−) of 100 μM SDS and 10 μM GTPγS, membranes were isolated from each incubation mixture by sucrose gradient centrifugation and proteins were pelleted down with 20% TCA (v/v) before solubilization in sample buffer. Ten percent SDS–PAGE was then performed and fractionated proteins were blotted onto nitrocellulose. The transferred proteins were incubated with rabbit antisera raised against p47*phox* and p67*phox* and immune complexes were revealed by chemiluminescence reaction. This result is representative of three separate experiments.

### 3.5. Translocation of p47phox and p67phox to neutrophil membranes in a cell-free oxidase reconstitution assay

To investigate the functional effect of the double substitution at residues 303 and 304 of gp91*phox*, we checked the ability of the cytosolic factors to be translocated to the membrane-bound cytochrome $b_{558}$, using an in vitro translocation assay. In a control experiment (Fig. 6), cytosolic activating factors p47*phox* and p67*phox* translocated to neutrophil membranes; this was fully dependent on the presence of SDS and GTPγS. On the contrary, with the case of patient JR, translocation of p47*phox* and p67*phox* to neutrophil membranes was hardly detectable. In addition, no translocation of the cytosolic factors was detected when the fraction originated from an $X91^0$ CGD patient, which confirms that in the absence of cytochrome $b_{558}$ no translocation of p67*phox* and p47*phox* could occur.

### 3.6. Effect of peptide 296–309 of gp91phox on NADPH oxidase assembling

To determine whether the gp91*phox* mutated domain of patient JR's neutrophils was directly in-

volved in the binding of the cytosolic factors p47*phox* and p67*phox*, experiments with synthetic peptides were performed. Two peptides were used (final concentration from 0 to 60 μM): one with a normal sequence 296–309 (wild-type peptide) and the other from the same region with the double amino acid substitution (mutated peptide), mimicking the mutation present in gp91*phox* of neutrophils from patient JR. The effect of these two peptides on NADPH oxidase activity was tested in a cell-free assay. No inhibition of NADPH oxidase activity was observed with both (wild-type and mutated) peptides. On the contrary, the peptide 491–504 used by Leusen et al. [36] inhibited the NADPH oxidase activity reconstituted in the same conditions (data not shown).

## 4. Discussion

In this paper we report two identical rare X-linked CGD cases in which cytochrome $b_{558}$ is present at a normal level as measured by immunoblotting and difference absorption spectra while neutrophils fail to produce superoxide anions. Mutations were localized by single-strand conformational polymorphism analysis of amplified cDNA fragments corresponding to the gp91*phox* protein of CGD patients JR and VV. Sequence analysis of the mutated cDNA fragment showed two C-to-A and C-to-G base mutations at positions 919 and 923, predicting amino acid substitutions in the gp91*phox* cytoplasmic C-terminal tail at residues 303 and 304: both mutations correspond to the replacement of histidine by asparagine and of proline by arginine. The double mutation was identified in gp91*phox* RNA and in the *CYBB* gene purified from native mononuclear cells and from EBV-immortalized B lymphocytes of both patients. The mutations were genetically transmitted from the DNA of both mothers (who were sisters) and were localized in exon 9. The resulting defective NADPH oxidase activity originates from a rare X91$^+$ CGD type.

Fourteen other cases of X91$^+$ CGD have been reported (for review see [1]) and sometimes the inactivating mutations have provided interesting information about oxidase activation mechanisms. Seven of these X91$^+$ CGD cases have been studied for their functional properties and five of them are localized in the C-terminal tail of gp91*phox*. Recently Lausen and colleagues [37] described four novel X$^+$ CGD mutations. Three of them (Cys369→Arg, Gly408→Glu, and Glu568→Lys) substantially disturbed the association of p47*phox* and p67*phox* with the plasma membrane. Two of them, Cys369→Arg and Thr341→Lys are located in the putative FAD-binding domain of gp91*phox*. Apparently a strong relationship exists between the gp91*phox* domains involved in the electron transfer and the binding of cytosolic factors. The missense mutation Asp-500→Gly, situated in the external loop at the 3′ end of gp91*phox* according to previous structural studies [56], but not in the FAD or NADPH binding sites, leads to a translocation defect of the cytosolic factors to the membrane [36]. Surprisingly, a deletion of amino acids 488–497 described in an X$^+$CGD patient, which is indeed localized in this external cytosolic loop, does not affect cytosolic factor assembly to the plasma membrane [35]. An X91$^-$ has been described by Kaneda et al. [42] with a missense mutation in a site very close to our double mutation, changing Glu309 to Lys. In that case, the $O_2^-$ production was shown to be diminished and related to a low amount of cytochrome $b_{558}$; no information about FAD content and cytosolic factor translocation was reported. In patients JR and VV, the mutated region was localized in a site close to the putative FAD-binding domain of gp91*phox*. The FAD content of neutrophil plasma membranes from both patients and their parents was compared to values obtained with control plasma membranes. A normal amount of FAD was found in patient JR, his mother, and his father ($84 \pm 14$, $105 \pm 35$, and $104 \pm 10$, respectively). These results are in accordance with conclusions drawn from homology studies with ferrodoxin-NADP$^+$ reductase [9–11], showing that NADPH and FAD-binding domains are probably localized in a region downstream of His303 and Pro304. Moreover, the HPFT motif residues of gp91*phox*, which belong to the putative FAD-binding site, has recently been shown to be a good candidate for binding FAD, highlighting an essential role of His338 in this function [57]. This mutation seemed to affect the stability of the gp91*phox* subunit because only one third of the heme was present in the CGD patient while translocation of cytosolic proteins p67*phox* and p47*phox* occurred normally.

The mutations we report in this paper also provide interesting observations regarding the $H^+$ channel function of gp91*phox*. Because the mutated cytochrome retains the histidine motif critical for $H^+$ transport, the hemoprotein of both patients (JR and VV) was expected to still function as an $H^+$ channel. As shown in Fig. 5, $H^+$ conductance could readily be detected in EBV-transformed B lymphocytes from patient JR. Surprisingly however, the mutated cytochrome was still able to catalyze inward $H^+$ fluxes and to generate a cytosolic acidification upon stimulation with arachidonic acid. In previous patch-clamp studies [16,17], inward $H^+$ currents were observed in phagocytes only in conditions that allow the assembly of a fully functional oxidase. Contrary to the lack of inward $H^+$ fluxes reported in cells from an $X91^0$ patient [58], the presence of a normal cytosolic acidification in cells from patient JR, which are not able to assemble a functional oxidase, indicates that the mutated cytochrome is still fully functional as an $H^+$ channel. Thus, these results suggest that the $H^+$ channel function requires neither the assembly nor the redox function of the oxidase, consistent with gp91*phox* itself being a fully functional $H^+$ channel.

Although interactions among the cytosolic factors and between these factors and the light chain of cytochrome $b_{558}$ p22*phox*, are well defined (for review see [2]), interacting domains between gp91*phox* and the other proteins of the NADPH oxidase complex are uncertain. The cell-free translocation of cytosolic p47*phox* and p67*phox* to patient JR's neutrophil plasma membrane was investigated and compared to that obtained with neutrophil membranes from a healthy donor. In control experiments, assembling occurred normally (Fig. 6), while in the CGD patients JR and VV, there was no translocation of the cytosolic activating factors despite the presence of the redox component of NADPH oxidase.

To investigate the direct implication of the mutated region of gp91*phox* in the assembly process, competitive experiments in the $O_2^-$-generating cell-free system were carried out with wild-type and mutated synthetic peptides corresponding to the sequence 296–309 of gp91*phox*. No inhibition of NADPH oxidase activity was observed with either (wild-type and mutated) peptide. On the contrary, the peptide 491–504 used by Leusen et al. [36] inhibited the NADPH oxidase activity reconstituted in the same conditions (data not shown). This suggests that Asp500 in gp91*phox* is directly implicated in the association of cytosolic factors p47*phox* and p67*phox* proteins with gp91*phox* and that the gp91*phox* mutated region of patient JR is probably not directly involved in the binding of the cytosolic factors, even if this domain is crucial in the NADPH oxidase assembling. The identified double missense mutation leading to the transformation of an His to an Asp and of a Pro to an Arg results in a change in the amino acid residue charges; this could explain a conformational modification of gp91*phox* and the lack of assembling.

Only one double missense mutation was reported in the *NCF2* gene encoding p67*phox* resulting in a CGD disease [59]. In that case the patient was heterozygous for the double mutation according to the genomic DNA analysis and the p67*phox* protein was not expressed. This double missense mutation was found in homozygous state when the corresponding RT–PCR fragment was sequenced. Probably the *NCF2* second allele carried another mutation not described by the authors, leading to an unstable mRNA. A very rare (T. Shoshani, N. Basham, B. Kerem, March 21, 1991) double missense mutation was reported in the *CFTR* gene described in the cystic fibrosis (CF) mutation data base (www.genet.sickkids;on.ca/cftr-cgi-bin) containing 996 described mutations. In the latter observation, both mutations were discovered together on six CF chromosomes, from three unrelated Jewish CF families from Georgia in eastern Europe. The CF children in these families were homozygous for these two mutations. We can conclude that a double missense mutation can occur but it seems to be very rare. At that time, we did not know whether one of the two mutations in the CGD patients JR and VV was a polymorphism that had appeared quite recently. The probability that both missense mutations occurred at the same time is very low; the evidence of a polymorphism for one mutation cannot be excluded and further experiments are needed to address the question. However, His303 and Pro304 seem to play an important role in the NADPH oxidase activity because they are preserved in all Nox analogs [60] except His303 in Nox 5.

## Acknowledgements

We are grateful to Professor P.V. Vignais and Dr. I. de Mendez for critical reading of the manuscript and helpful suggestions. We also thank Dr. D. Roos and Dr. A.J. Verhoeven for the generous gift of mAb449 and mAb48 antibodies raised against the two subunits of cytochrome $b_{558}$. We thank Dr. M. Dinauer for information on the *CYBB* gene, Mr. C. Castelbou for skillful technical help. We also thank Ms. Linda Northrup for correction of the English. Supported by grants from the Université Joseph Fourier, Faculté de Médecine; the Région Rhône-Alpes, programme Emergence; the Ministère de l'Education et de la Recherche, MENRT; and the Direction Régionale de la Recherche Clinique, DRRC.

## References

[1] B.M. Babior, NADPH oxidase: an update, Blood 93 (1999) 1464–1476.
[2] F.R. De Leo, M.T. Quinn, Assembly of the phagocyte NADPH oxidase: Molecular interaction of oxidase proteins, J. Leukocyte Biol. 60 (1996) 677–691.
[3] A. Abo, E. Pick, A. Hall, N. Totty, C.G. Teahan, A.W. Segal, Activation of the NADPH oxidase involves the small GTP-binding protein p21rac, Nature 353 (1991) 668–670.
[4] U.G. Knaus, P.P. Heyworth, B.T. Kinsella, J.T. Curnutte, G.M. Bokoch, Purification and characterization of Rac 2. A cytosolic GTP-binding protein that regulates human neutrophil NADPH oxidase, J. Biol. Chem. 267 (1992) 23575–23582.
[5] R.A. Clark, B.D. Volpp, K.G. Leidal, W.M. Nauseef, Two cytosolic components of the human neutrophil respiratory burst oxidase translocate to the plasma membrane during cell activation, J. Clin. Invest. 85 (1990) 714–721.
[6] D.R. Ambruso, B.G.J.M. Bolscher, P.M. Stokman, A.J. Verhoeven, D. Roos, Assembly and activation of the NADPH:$O_2$ oxidoreductase in human neutrophils after stimulation with phorbol myristate acetate, J. Biol. Chem. 265 (1991) 924–930.
[7] F.B. Wientjes, J.J. Hsuan, N.F. Totty, A.W. Segal, p40phox, a third cytosolic component of the activation complex of the NADPH oxidase contain src homology 3 domains, Biochem. J. 296 (1993) 557–561.
[8] A.R. Cross, J. Rae, J.T. Curnutte, Cytochrome $b_{-245}$ of neutrophil superoxide-generating system contains two non-identical hemes. Potentiometric studies of a mutant form of gp91phox, J. Biol. Chem. 270 (1995) 17075–17077.
[9] A.W. Segal, I. West, F. Wientjes, J.H.A. Nugent, A.J. Chavan, B. Haley, R.C. Garcia, H. Rosen, G. Scrace, Cytochrome $b_{-245}$ is a flavocytochrome containing FAD and the NADPH-binding site of microbicidal oxidase of phagocytes, Biochem. J. 284 (1992) 781–788.
[10] H. Sumimoto, N. Sakamoto, M. Nozaki, Y. Sakaki, K. Takeshige, S. Minakami, Cytochrome $b_{558}$, a component of phagocyte NADPH oxidase is a flavoprotein, Biochem. Biophys. Res. Commun. 186 (1992) 1368–1375.
[11] D. Rotrosen, C.L. Yeung, T.L. Leto, H.M. Malech, C.H. Kwong, Cytochrome $b_{558}$: The flavin-binding component of the phagocyte NADPH oxidase, Science 256 (1992) 1459–1462.
[12] J. Doussière, A. Poinas, C. Blais, P.V. Vignais, Phenylarsine oxide as an inhibitor of the activation of the neutrophil NADPH oxidase, Identification of the b subunit of the cytochrome *b* component of the NADPH oxidase as a target site for phenylarsine oxide by photoaffinity labeling and photoinactivation, Eur. J. Biochem. 251 (1998) 649–658.
[13] J. Doussière, G. Buzenet, P.V. Vignais, Photoaffinity labeling and photoinactivation of the $O_2^-$-generating oxidase of neutrophils by an azido derivative of FAD, Biochemistry 34 (1995) 1760–1770.
[14] L.M. Henderson, J.B. Chappel, NADPH oxidase of neutrophils, Biochim. Biophys. Acta 1273 (1996) 87–107.
[15] A. Nanda, R. Romanek, J.T. Curnutte, S. Grinstein, Assessment of the contribution of the cytochrome *b* moiety of the NADPH oxidase to the transmembrane $H^+$ conductance of leukocytes, J. Biol. Chem. 269 (1994) 27280–27285.
[16] B. Banfi, J. Schrenzel, O. Nusse, D.P. Lew, E. Ligeti, K.H. Krause, N. Demaurex, A novel $H^+$ conductance in eosinophils: unique characteristics and absence in chronic granulomatous disease, J. Exp. Med. 190 (1999) 183–194.
[17] T.E. DeCoursey, V.V. Cherny, W. Zhou, L.L. Thomas, Simultaneous activation of NADPH oxidase-related proton and electron currents in human neutrophils, Proc. Natl. Acad. Sci. USA 97 (2000) 6885–6889.
[18] L.M. Henderson, J.B. Chappel, O.T. Jones, The superoxide-generating NADPH oxidase of human neutrophils is electrogenic and associated with an $H^+$ channel, Biochem. J. 246 (1987) 325–329.
[19] L.M. Henderson, G. Banting, J.B. Chapell, The arachidonate-activable, NADPH oxidase-associated $H^+$ channel. Evidence that gp91-phox functions as an essential part of the channel, J. Biol. Chem. 207 (1995) 5909–5916.
[20] L.M. Henderson, S. Thomas, G. Banting, J.B. Chapell, The arachidonate-activable, NADPH oxidase-associated $H^+$ channel is contained within the multi-membrane-spanning N-terminal region of gp91-phox, Biochem. J. 325 (Pt. 3) (1997) 701–705.
[21] L.M. Henderson, Role of histidines identified by mutagenesis in the NADPH oxidase-associated $H^+$ channel, J. Biol. Chem. 273 (1998) 33216–33223.
[22] B. Banfi, A. Maturana, S. Jaconi, S. Arnaudeau, T. Laforge, B. Sinha, E. Ligeti, N. Demaurex, K.H. Krause, A mammalian $H^+$ channel generated through alternative splicing of the NADPH oxidase homolog NOH-1, Science 287 (2000) 138–142.

[23] B. Banfi, G. Molnar, A. Maturana, K. Steger, B. Hegedus, N. Demaurex, K.H. Krause, A Ca (2+)-activated NADPH oxidase in testis, spleen, and lymph nodes, J. Biol. Chem. 276 (2001) 37594–37601.
[24] A. Maturana, S. Arnaudeau, S. Ryser, B. Banfi, J.P. Hossle, W. Schlegel, K.H. Krause, N. Demaurex, Heme histidine ligands within gp91phox modulate proton conduction by the phagocyte NADPH oxidase, J. Biol. Chem. 276 (2001) 30277–30284.
[25] F. Morel, F. Boulay, J. Doussière, P.V. Vignais, Bases moléculaires de la granulomatose septique, Méd. Sci. 8 (1992) 912–920.
[26] J.T. Curnutte, Chronic granulomatous disease: the solving of a clinical riddle at the molecular level, Clin. Immunol. Immunopathol. 67 (1993) S2–S15.
[27] A.W. Segal, The NADPH oxidase and chronic granulomatous disease, Mol. Med. Today 2 (1996) 129–135.
[28] B. Royer-Pokara, L.M. Kunkel, A.P. Monaco, S.C. Goff, P.E. Newburger, R.L. Baehner, F.S. Cole, J.T. Curnutte, S.H. Orkin, Cloning the gene for an inherited human disorder – chronic granulomatous disease – on the basis of its chromosomal location, Nature 322 (1986) 32–38.
[29] T. Ariga, M. Nakanishi, K. Tomizawa, S. Imajoh-Ohmi, S. Kanegasaki, Y. Sakiyama, S. Matsumoto, Genetic heterogeneity in patients with X-linked chronic granulomatous disease, Pediatr. Res. 31 (1992) 516–519.
[30] D. Roos, M. de Boer, F. Kuribayashi, C. Meischl, R.S. Weening, A.W. Segal, A. Ahlin, K. Nemet, J.P. Hossle, E. Bernatowska-Matuszkiewicz, H. Middleton-Price, Mutation in the X-linked and autosomal recessive forms of chronic granulomatous disease, Blood 87 (1996) 1663–1681.
[31] B.M. Segal, T.L. Leto, J.I. Gallin, H.L. Malech, S.M. Holland, Genetic and clinical features of chronic granulomatous disease, Medicine 79 (2000) 170–200.
[32] T. Ariga, Y. Sakiyama, K. Tomizawa, S. Imajoh-Ohmi, S. Kanegasaki, S. Matsumoto, A newly recognized point mutation in the cytochrome $b_{558}$ heavy chain gene replacing alanine 57 by glutamic acid, in a patient with cytochrome *b* positive chronic granulomatous disease, Eur. J. Pediatr. 152 (1993) 469–472.
[33] A.R. Cross, P.G. Heyworth, J. Rae, J.T. Curnutte, A variant X-linked chronic granulomatous disease patient ($X91^+$) with partially functional cytochrome *b*, J. Biol. Chem. 270 (1995) 8194–8200.
[34] H. Azuma, H. Oomi, K. Sasaki, I. Kawabata, T. Sakaino, S. Koyano, T. Suzutani, H. Nuoi, A. Okuno, A new mutation in exon 12 of the gp91-phox gene leading to cytochrome *b*-positive X-linked chronic granulomatous disease, Blood 85 (1995) 3274–3277.
[35] L. Yu, A.R. Cross, L. Zhen, M.C. Dinauer, Functional analysis of NADPH oxidase in granulocytic cells expressing a Δ488-497 gp91phox deletion mutant, Blood 94 (1999) 2497–2504.
[36] J.H.W. Leusen, M. de Boer, G.J.M. Bolscher, P.M. Hilarius, R.S. Weening, H.D. Ochs, D. Roos, A.J. Verhoeven, A point mutation in gp91-phox of cytochrome $b_{558}$ of the human NADPH oxidase leading to defective translocation of the cytosolic proteins p47-phox and p67-phox, J. Clin. Invest. 93 (1994) 2120–2126.
[37] J.H.W. Leusen, C. Meischl, M.H.M. Eppink, P.M. Hilarius, M. de Boer, R.S. Weening, A. Ahlin, L. Sanders, D. Goldblatt, H. Skopczynska, E. Bernatowska, J. Palmblad, A.J. Verhoeven, W.J.H. van Berkel, D. Roos, Four novel mutations in the gene encoding gp91-phox of human NADPH oxidase: consequences for oxidase assembly, Blood 95 (2000) 666–673.
[38] M.C. Dinauer, J.T. Curnutte, H. Rosen, S.H. Orkin, A missense mutation in the neutrophil cytochrome *b* heavy chain in cytochrome-positive X-linked chronic granulomatous disease, J. Clin. Invest. 84 (1989) 2012–2016.
[39] V. Jendrossek, A. Ritzel, B. Neubauer, S. Heyden, M. Gahr, An in-frame triplet deletion within the gp91-phox gene in an adult X-linked chronic granulomatous disease patient with residual NADPH-oxidase activity, Eur. J. Haematol. 58 (1997) 78–82.
[40] J. Rae, P.E. Newburger, M.C. Dinauer, D. Noack, P.J. Hopkins, R. Kuruto, J.T. Curnutte, X-Linked chronic granulomatous disease: mutations in the CYBB gene encoding the gp91-phox component of respiratory-burst oxidase, Am. J. Hum. Genet. 62 (1998) 1320–1325.
[41] J. Roesler, S. heyden, M. Burdelski, H. Schafer, H.W. Kreth, R. Lehmann, D. Paul, J. Marzahn, M. Gahr, A. Rosen-Wolff, Uncommon missense and splice mutations and resulting biochemical phenotypes in German patients with X-linked chronic granulomatous disease, Exp. Hematol. 27 (1999) 505–511.
[42] M. Kaneda, H. Sakuraba, A. Ohtake, A. Nishida, C. Kiryu, A. Kakinuma, Missense Mutations in the gp91-phox gene encoding cytochrome $b_{558}$ in patients with cytochrome *b* positive and negative X-linked chronic granulomatous disease, Blood 93 (1999) 2098–2104.
[43] A. Böyum, Isolation of mononuclear cells and granulocytes from human blood, Scand. J. Clin. Lab. Invest. 21 (Suppl. 97) (1968) 77–89.
[44] L. Cohen-Tanugi, F. Morel, M.C. Pilloud-Dagher, J.M. Seigneurin, P. François, M. Bost, P.V. Vignais, Activation of $O_2^-$-generating oxidase in an heterologous cell-free system derived from Epstein–Barr-virus-transformed human B lymphocytes and bovine neutrophils, Eur. J. Biochem. 202 (1991) 649–655.
[45] P. Chomczynski, N. Sacchi, Single-step method of RNA isolation by acid guanidium thiocyanate-phenol-chloroform extraction, Anal. Biochem. 162 (1987) 156–159.
[46] J. Bell, J.H. Karam, W.J. Rutter, Polymorphic DNA region adjacent to 5′ end of human insulin gene, Proc. Natl. Acad. Sci. USA 78 (1981) 5759–5763.
[47] M. Orrita, H. Iwahana, H. Kanazawa, K. Hayashi, T. Sekiya, Detection of polymorphisms of human DNA by gel electrophoresis as single-strand conformation polymorphisms, Proc. Natl. Acad. Sci. USA 86 (1989) 2766–2770.
[48] G. Batot, M.H. Paclet, J. Doussière, S. Vergnaud, C. Martel, P.V. Vignais, F. Morel, Biochemical and immunochemical

properties of B lymphocyte cytochrome $b_{558}$, Biochim. Biophys. Acta 1406 (1998) 188–202.
[49] F. Morel, J. Doussière, M.J. Stasia, P.V. Vignais, The respiratory burst of bovine neutrophils. Role of *b* type cytochrome and coenzyme specificity, Eur. J. Biochem. 152 (1985) 669–679.
[50] L.S. Yoshida, T. Chiba, K. Kakinuma, Determination of flavin contents in neutrophils by a sensitive chemiluminescence assay: evidence for no translocation of flavoproteins from the cytosol to the membrane upon cell stimulation, Biochim. Biophys. Acta 1135 (1992) 245–252.
[51] U.K. Laemmli, Cleavage of structural proteins during the assembly of the head of bacteriophage T4, Nature 227 (1970) 680–685.
[52] H. Towbin, T. Staehelin, J. Gordon, Electrophoretic transfer of proteins from polyacrylamide gels to nitrocellulose sheets: procedure and some application, Proc. Natl. Acad. Sci. USA 76 (1979) 4350–4354.
[53] A.J. Verhoeven, G.J.M. Bolscher, L. Meerhof, R. van Zwieten, J. Keijer, R.S. Weening, D. Roos, Characterization of two monoclonal antibodies against cytochrome $b_{558}$ of human neutrophils, Blood 73 (1989) 1686–1694.
[54] S. Vergnaud, M.H. Paclet, J. El Benna, M.A. Pocidalo, F. Morel, Complementation of NADPH oxidase in p67-phox/p40-phox interaction, Eur. J. Biochem. 267 (2000) 1059–1067.
[55] M.M. Bradford, A rapid and sensitive method for quantitation of microgram quantities of protein utilizing the principle of protein–dye binding, Anal. Biochem. 72 (1976) 248–254.
[56] W.R. Taylor, D.T. Jones, A.W. Segal, A structural model for nucleotide binding domains of the flavocytochrome $b_{-245}$ beta-chain, Protein Sci. 2 (1993) 1675–1685.
[57] L.S. Yoshida, F. Saruka, K. Yoshikawa, O. Tatsuzawa, S. Tsunawaki, Mutation at Histidine 338 of gp91phox depletes FAD and affects expression of cytochrome $b_{558}$ of human NADPH oxidase, J. Biol. Chem. 43 (1998) 27879–27886.
[58] A. Nanda, S. Grinstein, J.T. Curnutte, Abnormal activation of $H^+$ conductance in NADPH oxidase-defective neutrophils, Proc. Natl. Acad. Sci. USA 90 (1993) 760–764.
[59] A. Bonizzato, M.P. Russo, M. Donini, S. Dusi, Identification of a double mutation (D160V-K161E) in the p67phox gene of a chronic granulomatous disease patient, Biochem. Biophys. Res. Commun. 231 (1997) 861–863.
[60] G. Cheng, Z. Cao, X. Xu, E.G. Van Meir, J.D. Lambeth, Homologs of gp91phox: cloning and tissue expression of Nox3, Nox 4, and Nox 5, Gene 269 (2001) 131–140.